Chemistry of Polynuclear Metal Complexes with Bridging Carbene or Carbyne Ligands. Part 88.[1] Carbaboranetungsteniridium Compounds; Crystal Structure of the Complex $[WIr(\mu\text{-}CC_6H_4Me\text{-}4)(CO)_2(PEt_3)_2(\eta^5\text{-}C_2B_9H_9Me_2)]$*

John C. Jeffery, Miguel A. Ruiz, Paul Sherwood, and F. Gordon A. Stone
Department of Inorganic Chemistry, The University, Bristol BS8 1TS

The reaction between the compounds $[Ir(PPh_3)_2(cod)][PF_6]$ (cod = cyclo-octa-1,5-diene) and $[N(PPh_3)_2][W(\equiv CR)(CO)_2(\eta^5\text{-}C_2B_9H_9Me_2)]$ (R = C_6H_4Me-4) in thf (tetrahydrofuran) at room temperature affords the complex $[WIr(\mu\text{-}CR)(CO)_2(PPh_3)_2(\eta^5\text{-}C_2B_9H_9Me_2)]$. The triphenylphosphine groups in the latter can be displaced with PEt_3, $P(OPh)_3$, or $P(OMe)_3$ to give the compounds $[WIr(\mu\text{-}CR)(CO)_2L(L')(\eta^5\text{-}C_2B_9H_9Me_2)]$ [L = L' = PEt_3, $P(OPh)_3$, or $P(OMe)_3$; L = PPh_3, L' = $P(OMe)_3$]. In solution several of these products exist as isomeric mixtures. An *X*-ray diffraction study was carried out on an isomer of $[WIr(\mu\text{-}CR)(CO)_2(PEt_3)_2(\eta^5\text{-}C_2B_9H_9Me_2)]$. The W–Ir bond [2.590(1) Å] is spanned by the *p*-tolylmethylidyne group [μ-C–W 2.06(1), μ-C–Ir 1.95 (1) Å]. The *nido*-icosahedral fragment $C_2B_9H_9Me_2$ is η^5-co-ordinated to the tungsten, but the central boron CCB*B*B in the pentagonal face of the ligand is attached to the iridium *via* a two-electron three-centre B–H→Ir bond. The tungsten atom also carries two terminal CO groups, and the two PEt_3 ligands are bonded to the iridium. The co-ordination environment of the iridium is such that the plane defined by the atoms IrP_2 is perpendicular to that containing the atoms W, μ-C, and B–H→Ir, and the midpoint of the cage C–C bond. The reaction between $[WIr(\mu\text{-}CR)(CO)_2(PPh_3)_2(\eta^5\text{-}C_2B_9H_9Me_2)]$ and $P(OMe)_3$ also affords the compounds $[WIrH(\mu\text{-}CR)(\mu\text{-}\sigma\text{:}\eta^5\text{-}C_2B_9H_8Me_2)(CO)_3\{P(OMe)_3\}_2]$ and $[WIrH\{\mu\text{-}\sigma\text{:}\eta^5\text{-}CH(R)(C_2B_9H_7Me_2)\}(CO)_2\{P(OMe)_3\}_4]$. Similarly PMe_3 displaces the PPh_3 groups in the precursor to give $[WIrH(\mu\text{-}CR)(\mu\text{-}\sigma\text{:}\eta^5\text{-}C_2B_9H_8Me_2)(CO)_2(PMe_3)_3]$ and $[WIrH\{\mu\text{-}\sigma\text{:}\eta^5\text{-}CH(R)(C_2B_9H_7Me_2)\}(CO)_2(PMe_3)_4]$. The reactions between $[IrL_2(cod)][PF_6]$ (L_2 = $Ph_2PCH_2CH_2PPh_2$ or 2,2′-bipyridine) and $[N(PPh_3)_2][W(\equiv CR)(CO)_2(\eta^5\text{-}C_2B_9H_9Me_2)]$ yield tungsten–iridium complexes $[WIrH(\mu\text{-}CR)(\mu\text{-}\sigma\text{:}\eta^5\text{-}C_2B_9H_8Me_2)(CO)_3L_2]$ with terminal Ir–H bonds, and σ B–Ir linkages to the carbaborane group ligating the tungsten. N.m.r. data (^1H, ^{13}C-{^1H}, ^{31}P-{^1H}, and ^{11}B-{^1H}) for the new compounds are reported and discussed.

In this paper we report the synthesis of several compounds containing W–Ir bonds. These studies form part of a broader investigation in which the anionic complexes $[W(\equiv CR)(CO)_2(\eta^5\text{-}C_2B_9H_9Me_2)]^-$ (R = alkyl or aryl) are used as reagents for preparing species with heteronuclear metal–metal bonds.[2] In our initial work in this area[3] we synthesised the compounds $[WRh(\mu\text{-}CC_6H_4Me\text{-}4)(CO)_2L_2(\eta^5\text{-}C_2B_9H_9Me_2)]$ [L = PPh_3 (**1a**) or L_2 = dppe ($Ph_2PCH_2CH_2PPh_2$) (**1b**)] by treating $[Rh(PPh_3)_2(cod)][PF_6]$ or $[Rh(dppe)(cod)][PF_6]$ (cod = cyclo-octa-1,5-diene) respectively, with $[N(PPh_3)_2][W(\equiv CC_6H_4Me\text{-}4)(CO)_2(\eta^5\text{-}C_2B_9H_9Me_2)]$. Moreover, it was also observed that addition of PEt_3 to (**1a**) displaced the PPh_3 groups and afforded $[WRh(\mu\text{-}CC_6H_4Me\text{-}4)(CO)_2(PEt_3)_2(\eta^5\text{-}C_2B_9H_9Me_2)]$ (**1c**). In these tungsten–rhodium compounds the carbaborane group adopts its normal spectator role as found in numerous carbametallaboranes. However, subsequent work with salts of the anions $[W(\equiv CR)(CO)_2(\eta^5\text{-}C_2B_9H_9Me_2)]^-$ revealed that the results obtained with the rhodium compounds were atypical. A much more common feature of reactions of this type, and one which makes them particularly interesting, is that the *nido*-icosahedral C_2B_9 fragment ligating the tungsten atom forms exopolyhedral linkages with adjacent groups *via* boron atoms in the $\eta^5\text{-}C_2B_3$ face of the cage.[4] Most commonly a three-centre two-electron B–H→M bond is formed from the cage to

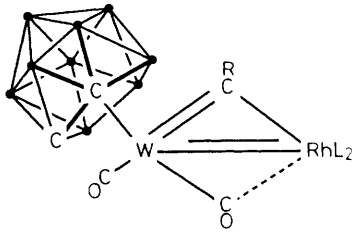

C = CMe • = BH R = C_6H_4Me-4

	L	L_2
(**1a**)	PPh_3	
(**1b**)		dppe
(**1c**)	PEt_3	

the transition element (M) attached to the tungsten. Typical of products known to contain this structural feature are the compounds $[WRu(\mu\text{-}CC_6H_4Me\text{-}4)(CO)_3(\eta\text{-}C_5H_5)(\eta^5\text{-}C_2B_9H_9Me_2)]$,[4a] $[WMo(\mu\text{-}CC_6H_4Me\text{-}4)(CO)_3(\eta^5\text{-}C_9H_7)(\eta^5\text{-}C_2B_9H_9Me_2)]$ ($\eta^5\text{-}C_9H_7$ = indenyl),[4b] $[NEt_4][WCo_2(\mu_3\text{-}CPh)(CO)_6(\eta^5\text{-}C_2B_9H_9Me_2)]$,[4c] and $[WPtH(\mu\text{-}CC_6H_3Me_2\text{-}2,6)(CO)_2(PEt_3)(\eta^5\text{-}C_2B_9H_9Me_2)]$.[2] However, species having these B–H→M linkages often serve as intermediates on a pathway to other complexes, formed either directly or upon addition of another reagent, such as CO, PMe_3, H^-, or an alkyne. Thus compounds with B–M σ bonds

* *Supplementary data available:* see Instructions for Authors, *J. Chem. Soc., Dalton Trans.*, 1989, Issue 1, pp. xvii—xx.

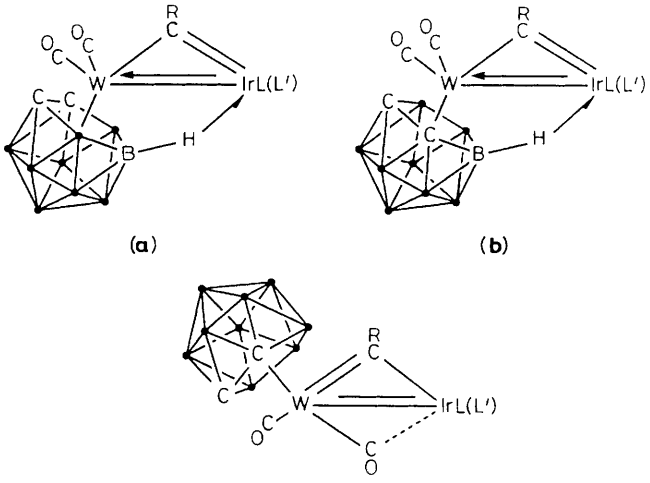

	L	L′
(**2**)	PPh_3	PPh_3
(**3**)	PEt_3	PEt_3
(**4**)	$P(OPh)_3$	$P(OPh)_3$
(**5**)	PPh_3	$P(OMe)_3$
(**6**)	$P(OMe)_3$	$P(OMe)_3$

are frequently isolated, *e.g.* $[WPt(\mu\text{-}CC_6H_3Me_2\text{-}2,6)(\mu\text{-}\sigma\text{:}\eta^5\text{-}C_2B_9H_8Me_2)(CO)_3(PEt_3)]$,[2] $[NEt_4][WFe\{\mu\text{-}CH(C_6H_4Me\text{-}4)\}(\mu\text{-}\sigma\text{:}\eta^5\text{-}C_2B_9H_8Me_2)(\mu\text{-}CO)(CO)_5]$,[5a] or $[WPt(\mu\text{-}H)\{\mu\text{-}\sigma\text{:}\eta^5\text{-}C_2B_9H_7(CH_2C_6H_4Me\text{-}4)Me_2\}(CO)_2(PMe_3)(PEt_3)_2]$.[5b] The fate of the alkylidyne moiety is of interest. It may remain as a bridging ligand spanning the two metal centres, it may be converted into an alkylidene group by hydrogen transfer from the B–H→M fragment, or it may be hydroborated becoming an alkyl substituent attached to one of the boron atoms in the $\eta^5\text{-}C_2B_3$ face of the carbaborane cage. In yet another pathway, however, the alkylidyne group inserts into the B–H→M fragment, generating a B–C bond and affording a bridging $\mu\text{-}CH(R)(C_2B_9H_8Me_2)$ moiety. The compounds $[MoW\{\mu\text{-}\sigma\text{:}\eta^3\text{-}CH(C_6H_4Me\text{-}4)(C_2B_9H_8Me_2)\}(CO)_3(\eta\text{-}EtC_2Et)(\eta^5\text{-}C_9H_7)]$[6] and $[WRu\{\mu\text{-}\sigma\text{:}\eta^5\text{-}CH(C_6H_4Me\text{-}4)(C_2B_9H_8Me_2)\}(CO)_3(PMe_3)(\eta\text{-}C_5H_5)]$[4a] are products which exemplify this reactivity pattern.

In view of these results the spectator role of the $\eta^5\text{-}C_2B_9H_9Me_2$ ligand in the complexes (**1**) is surprising. It was thought that corresponding reactions with iridium salts should be examined, since this metal when bonded to tungsten would be more likely than rhodium to activate the nearby carbaborane group. Reactions affording exopolyhedral B–H→M or B–M bonds correspond, respectively, to an incipient oxidative-addition or a formal oxidative-addition process. Such transformations are known to be more facile at an iridium centre than at rhodium.[7] A preliminary account of some of the results described herein has been given.[8]

Results and Discussion

The reaction between $[Ir(PPh_3)_2(cod)][PF_6]$ and $[N(PPh_3)_2][W(\equiv CC_6H_4Me\text{-}4)(CO)_2(\eta^5\text{-}C_2B_9H_9Me_2)]$ in thf (tetrahydrofuran) at room temperature gave the black-green compound $[WIr(\mu\text{-}CC_6H_4Me\text{-}4)(CO)_2(PPh_3)_2(\eta^5\text{-}C_2B_9H_9Me_2)]$ (**2**), data for which are summarised in Tables 1—3. Treatment of (**2**) in thf with an excess of PEt_3 afforded the red-brown complex $[WIr(\mu\text{-}CC_6H_4Me\text{-}4)(CO)_2(PEt_3)_2(\eta^5\text{-}C_2B_9H_9Me_2)]$ (**3**). The PPh_3 ligands in (**2**) could also be displaced by the tertiary phosphites $P(OPh)_3$ or $P(OMe)_3$, and in this manner the compounds $[WIr(\mu\text{-}CC_6H_4Me\text{-}4)(CO)_2L(L')(\eta^5\text{-}C_2B_9H_9Me_2)]$ [L = L′ = $P(OPh)_3$ (**4**); L = PPh_3, L′ = $P(OMe)_3$ (**5**); and L = L′ = $P(OMe)_3$ (**6**)] were obtained (Tables 1—3). The spectroscopic data for compounds (**2**)—(**6**) revealed that several of these species existed in solution as mixtures of isomers. Moreover, the nature of the isomers and their relative proportions were very solvent dependent.

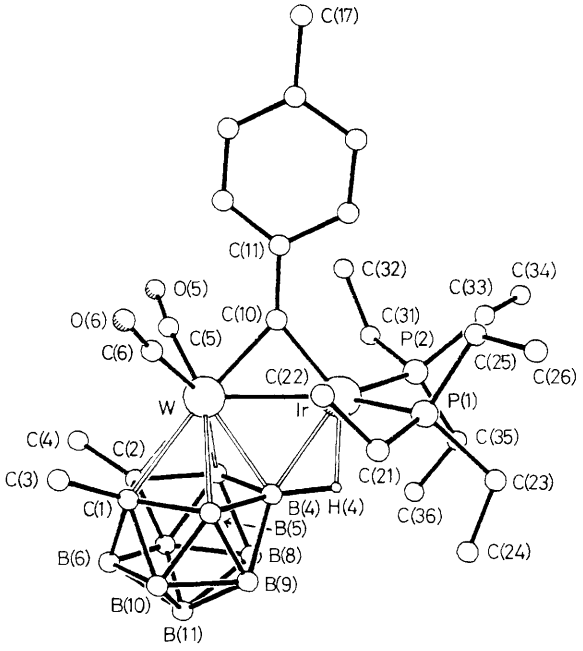

Figure. Molecular structure of the complex $[WIr(\mu\text{-}CC_6H_4Me\text{-}4)(CO)_2(PEt_3)_2(\eta^5\text{-}C_2B_9H_9Me_2)]$ (**3a**) showing the crystallographic numbering scheme

Fortunately, it was possible to grow crystals of (**3**) corresponding to a single isomer, and an *X*-ray diffraction study was carried out. The results are summarised in Table 4 and the structure is shown in the Figure.

It will be seen that the W–Ir bond is spanned by the *p*-tolylmethylidyne group, and that the carbaborane ligand on the tungsten forms an exopolyhedral B–H→Ir bond. The iridium atom is ligated by the atoms P(1), P(2), C(10), W, B(4), and H(4). Moreover, the plane defined by the atoms IrP(1)P(2) and that containing the atoms IrWC(10)B(4)H(4) and the midpoint of the C–C bond in the cage are essentially perpendicular to each other. The latter plane is one of non-crystallographic mirror symmetry, if the ethyl substituents on the phosphorus atoms are ignored.

The molecule may be viewed as resulting from a combination of the two fragments $[Ir(PEt_3)_2]^+$ and $[W(\equiv CC_6H_4Me\text{-}4)(CO)_2(\eta^5\text{-}C_2B_9H_9Me_2)]^-$, with the C≡W group in the latter formally contributing four electrons to the iridium centre.[9] However, several canonical forms can be written for the electron distribution in the μ-C(10)WIr ring system. Formulation (**3a**) is satisfying since it indicates a closed 18-electron shell at each metal centre, and is in accord with the observed W–Ir, C(10)–W, and C(10)–Ir separations discussed below.

The W–Ir bond length [2.590(1) Å] is sufficiently short to suggest multiple bonding between the two metal atoms. In the electronically saturated tungsten–iridium cluster compounds $[WIr_3(CO)_{11}(\eta\text{-}C_5H_5)]$ and $[W_2Ir_2(CO)_{10}(\eta\text{-}C_5H_5)_2]$ the metal–metal distances are significantly longer, being in the range 2.792(1)—2.865(1) Å.[10] The W–Ir separations in the

Table 1. Analytical[a] and physical data for the complexes

Compound[b]	Yield (%)	Colour	$\nu_{max.}$(CO)[c]/cm^{-1}			Analysis (%) C	H
(2) [WIr(μ-CR)(CO)$_2$(PPh$_3$)$_2$(η^5-C$_2$B$_9$H$_9$Me$_2$)]	78	Black-green	1 969vs,	1 903m,	1 740w (br)	49.0 (49.2)	4.8 (4.3)
(3) [WIr(μ-CR)(CO)$_2$(PEt$_3$)$_2$(η^5-C$_2$B$_9$H$_9$Me$_2$)]	82	Red-brown	1 963vs,	1 894s,	1 732vw (br)	33.4 (33.5)	5.9 (5.6)
(4) [WIr(μ-CR)(CO)$_2${P(OPh)$_3$}$_2$-(η^5-C$_2$B$_9$H$_9$Me$_2$)]	36	Yellow-green	1 985vs,	1 916s		46.5 (45.6)	4.1 (4.0)
(5) [WIr(μ-CR)(CO)$_2$(PPh$_3$){P(OMe)$_3$}-(η^5-C$_2$B$_9$H$_9$Me$_2$)]	46	Orange-brown	1 972vs,	1 905s		38.6 (38.8)	4.9 (4.3)
(6) [WIr(μ-CR)(CO)$_2${P(OMe)$_3$}$_2$(η^5-C$_2$B$_9$H$_9$Me$_2$)]	45	Orange	[d] 1 977vs,	1 912s		25.4 (25.5)	4.4 (4.3)
(7) [WIrH(μ-CR)(μ-σ:η^5-C$_2$B$_9$H$_8$Me$_2$)-(CO)$_3${P(OMe)$_3$}$_2$]	46	Yellow-brown	[e] 2 023w,	1 993vs,	1 900s	26.0 (26.0)	4.0 (4.2)
(8) [WIrH(μ-CR)(μ-σ:η^5-C$_2$B$_9$H$_8$Me$_2$)-(CO)$_2$(PMe$_3$)$_3$][f]	51	Green	1 974vw,	1 946s,	1 874vs		
(9) [WIrH(μ-CR)(μ-σ:η^5-C$_2$B$_9$H$_8$Me$_2$)-(CO)$_3$(dppe)]	50	Orange-brown	2 004m (sh), 1 901vs	1 991vs,	1 979s,	43.7 (43.9)	4.2 (4.1)
(10) [WIrH(μ-CR)(μ-σ:η^5-C$_2$B$_9$H$_8$Me$_2$)-(CO)$_3$(bipy)]	66	Brown	2 017m,	1 992vs,	1 908s	[g] 35.1 (34.1)	4.1 (3.4)
(11) [WIrH{μ-σ:η^5-CH(R)(C$_2$B$_9$H$_7$Me$_2$)}-(CO)$_2$(PMe$_3$)$_4$]	35	Orange	[h] 1 862vs,	1 762m		31.8 (31.2)	6.3 (5.9)
(12) [WIrH{μ-σ:η^5-CH(R)(C$_2$B$_9$H$_7$Me$_2$)}-(CO)$_2${P(OMe)$_3$}$_4$]	42	Orange	1 889vs,	1 855m		[i] 28.5 (28.5)	5.5 (5.3)

[a] Calculated values are given in parentheses. [b] R = C$_6$H$_4$Me-4. [c] In thf, unless otherwise stated. A broad band is observed in the range *ca.* 2 500—2 550 cm^{-1} due to ν(BH). [d] In light petroleum. [e] ν(IrH) at 2 140w (br) cm^{-1}. [f] Analytically pure sample not obtained. [g] N, 3.5 (3.2)%. [h] ν(IrH) at 2 145vw cm^{-1}. [i] Crystallised with a molecule of thf.

dimetal compounds [WIrH(μ-PPh$_2$)$_2$(CO)$_5$(PPh$_3$)] [2.876(1) Å] and [WIrH(μ-PPh$_2$)$_2${C(OMe)Ph}(CO)$_4$(PPh$_3$)] [2.858(1) Å] are also appreciably greater than that in (**3a**).[11]

The W–C(10) and Ir–C(10) distances in (**3a**) are also of interest. In several dimetal complexes containing dimetallacyclopropene ring systems W(μ-C)M (M = Pt, Co, Rh, Cr, or Ti), and in which a μ-C=W linkage is invoked, the carbon–tungsten separation is in the range 1.91(2)—2.03(1) Å.[12] The corresponding distance in (**3a**) [2.06(1) Å] is longer. In contrast with the somewhat lengthy W–C(10) bond, the Ir–C(10) distance [1.95(1) Å] lies between the ranges expected for a single and a double bond. For example, several methyliridium complexes have Ir–Me bond lengths in the range 2.13(2)—2.20(2) Å,[13] while the Ir=C bonds in the alkylidene complexes [Ir(=CH$_2$){N(SiMe$_2$CH$_2$PPh$_2$)$_2$}][14] and [Ir(=CCl$_2$)Cl$_3$(PPh$_3$)$_2$][15] are 1.868(9) and 1.872(7) Å in length, respectively.

The bridging hydrogen atom H(4), attached to the central boron in the pentagonal face of the cage ligating the tungsten, was located, but its position was not refined (see Experimental section). The geometric parameters of the B–H→Ir linkage are similar to those found for the two B–H→Rh bonds in [Rh$_2$(PPh$_3$)$_2$(η^5-C$_2$B$_9$H$_{11}$)$_2$].[16] The Ir–B(4) separation in (**3a**) [2.34(1) Å] is comparable with those in [Rh$_2$(PPh$_3$)$_2$(η^5-C$_2$B$_9$H$_{11}$)$_2$] [2.238(8) and 2.327(8) Å], but is shorter than the corresponding distances in [WRu(μ-CC$_6$H$_4$Me-4)(CO)$_3$(η-C$_5$H$_5$)(η^5-C$_2$B$_9$H$_9$Me$_2$)] [2.400(7) Å][4a] or [WMo(μ-CC$_6$H$_4$-Me-4)(CO)$_3$(η^5-C$_9$H$_7$)(η^5-C$_2$B$_9$H$_9$Me$_2$)] [2.49(2) Å],[4b] species which also contain B–H→M groups. Although the parameters for H(4) must be regarded as tentative, the B(4)–H(4) separation (1.2 Å) is as expected. The Ir–H(4) distance (1.8 Å) is close to the Rh–H separations [1.77(6) and 1.78(6) Å] observed in [Rh$_2$(PPh$_3$)$_2$(η^5-C$_2$B$_9$H$_{11}$)$_2$].[16]

The bond lengths from W to the atoms in the face of the carbaborane cage increase away from B(4) (Table 4). The slip distortion, defined as Δ,[17] is 0.21 Å, and probably serves to optimise the geometry of the B–H→Ir interaction. A slippage of similar magnitude has been observed in related structures.[4a,b] The Ir–P distances in (**3a**) are the same, and two CO groups attached to the tungsten are terminally bound to this atom.

Having established the structure of one isomer of (**3**) it was possible to attempt to interpret the relatively complicated spectroscopic properties of this species, determined from measurements in solution. The i.r. spectrum in the carbonyl stretching region when recorded in C$_6$H$_6$ showed two bands at 1 964vs and 1 895s cm^{-1}, and there was no absorption in the range expected for a bridging or semi-bridging CO ligand, as exists at 1 761 cm^{-1} in the spectrum of the rhodium analogue (**1c**).[3] The appearance of the two terminal CO stretches in C$_6$H$_6$ solutions of (**3**) thus seemed to be in accord with the structure (**3a**) established by *X*-ray diffraction. However, when the i.r. spectrum was measured in light petroleum, a solvent superior to C$_6$H$_6$ for resolving CO peaks, four terminal CO bands were observed at 1 974s, 1 969vs, 1 909s, and 1 903s cm^{-1}. This suggested the presence in non-polar solvents of two isomers (**3a**) and (**3b**) having very similar structures. The i.r. spectrum of (**3**) in thf was different again, with bands at 1 963vs, 1 894s, and 1 732w cm^{-1}. The latter peak was reminiscent of the low-frequency absorption in the spectrum of (**1c**), the structure of which has been established by *X*-ray diffraction.[3] The i.r. data for (**3**) obtained from thf solutions thus indicated the presence of a mixture of isomers one of which was (**3c**).

The n.m.r. data for complex (**3**) were also solvent dependent. The simplest spectra were recorded in C$_6$D$_6$, and like the i.r. measurements in C$_6$H$_6$ seemed to indicate, on the basis of the relatively few resonances observed, the presence of one isomer (**3a**). Thus there was a diagnostic resonance in the ^{1}H n.m.r. spectrum for a B–H→Ir group at δ −2.4 [*J*(BH) *ca.* 70 Hz],[2] and the ^{11}B-{^{1}H} n.m.r. spectrum also showed a characteristic signal for this group at δ 32.8 p.p.m., with the remaining ^{11}B nuclei giving rise to the usual broad peaks in the range −7.0 to −10.0 p.p.m.[4] In accord with the symmetrical structure of (**3a**), with a mirror plane through Ir, W, B(4), and the midpoint of C(1)–C(2) (Figure), the ^{31}P-{^{1}H} n.m.r. spectrum showed a single resonance, and the ^{1}H n.m.r. spectrum had one peak for the cage-methyl groups. An alternative explanation for the n.m.r. data, obtained from C$_6$D$_6$ or C$_6$D$_5$CD$_3$ solutions, is that they correspond not to the presence of a single isomer (**3a**), but to an averaging of peaks due to a rapid equilibration between

Table 2. Hydrogen-1 and carbon-13 n.m.r. data[a] for the complexes

Compound		$^1H(\delta)$[b]	$^{13}C(\delta)$[c]
(2)[d]	(a)	−1.6 (br, 1 H, B–H–Ir), 2.16 (s, 6 H, CMe), 2.46 (s, 3 H, Me-4), 7.0—7.4 (m, 34 H, C_6H_4 and Ph)	219.4 (CO), 160.5 [$C^1(C_6H_4)$], 137.6—125.0 (C_6H_4 and Ph), 63.5 (*C*Me), 32.1 (C*Me*), 21.5 (Me-4)
	(c)	1.80 (s, 6 H, CMe), 2.42 (s, 3 H, Me-4), 7.0—7.4 (m, 34 H, C_6H_4 and Ph)	340.5 (t, μ-C, *J*(PC) 12], 236.4 (CO), 152.5 [$C^1C_6H_4$)], 140.6—125.0 (C_6H_4 and Ph), 67.5 (*C*Me), 28.9 (C*Me*), 21.9 (Me-4)
(3)	(a)	[e] −2.4 [q br, 1 H, B–H–Ir, *J*(BH) 70], 0.90—1.80 (br, 30 H, Et), 2.12 (s, 3 H, Me-4), 2.28 (s, 6 H, CMe), 7.18, 8.09 [$(AB)_2$, 4 H, C_6H_4, *J*(AB) 7]	334.7 (br, μ-C), 219.3 [CO, *J*(WC) 165], 158.2 [$C^1(C_6H_4)$], 137.9, 129.1, 128.9 (C_6H_4), 62.1 (*C*Me), 32.3 (C*Me*), 22.3—21.2 (CH_2 and Me-4), 8.0 (*Me*CH_2P)
	(c)		334.2 [t, μ-C, *J*(PC) 12], 236.8 (CO), 152.6 [$C^1(C_6H_4)$], 139.7, 129.4, 126.5 (C_6H_4), 66.4 (*C*Me), 29.8 (C*Me*), 22.3—21.2 (CH_2 and Me-4), 8.3 (*Me*CH_2P)
(4)		−2.1 (br, 1 H, B–H–Ir), 2.01 (s, 6 H, CMe), 2.44 (s, 3 H, Me-4), 6.7—7.1 (m, 30 H, Ph), 7.41—8.67 (m, 4 H, C_6H_4)	334.2 [t, μ-C, *J*(PC) 14], 217.2 [CO, *J*(WC) 161], 151.8 [$C^1(C_6H_4)$], 151.5—120.9 (C_6H_4 and Ph), 63.6 (*C*Me), 32.0 (C*Me*), 22.0 (Me-4)
(5)		−2.3 [q br, 1 H, B–H–Ir, *J*(BH) 60], 2.22 (s, 6 H, CMe), 2.37 (s, 3 H, Me-4), 3.02 [d, 9 H, OMe, *J*(PH) 13], 7.23—7.32 (m, 15 H, Ph), 7.10, 7.59 [$(AB)_2$, 4 H, C_6H_4, *J*(AB) 7]	[f] 333.2 [d of d, μ-C, *J*(PC) 15, 7], 218.6 [d, CO, *J*(PC) 5], 217.7 (CO), 155.2 [$C^1(C_6H_4)$], 139.2—128.0 (C_6H_4 and Ph), 63.5, 63.0 (*C*Me), 52.5 [d, OMe, *J*(PC) 5], 32.0 (C*Me*), 21.8 (Me-4)
(6)		−2.1 (br, 1 H, B–H–Ir), 2.25 (s, 6 H, CMe), 2.39 (s, 3 H, Me-4), 3.25 (m, 18 H, OMe), 7.37, 8.89 [$(AB)_2$, 4 H, C_6H_4, *J*(AB) 8]	[f] 332.4 [t, μ-C, *J*(PC) 12], 217.2 (CO), 152.0 [$C^1(C_6H_4)$], 141.3, 137.5, 130.2 (C_6H_4), 63.2 (*C*Me), 53.1 (OMe), 32.1 (C*Me*), 22.1 (Me-4)
(7)		−12.52 [d of d, 1 H, HIr, *J*(PH), 18, 9], 2.08, 2.27, 2.50 (s × 3, 9 H, CMe and Me-4), 3.49, 3.64 [d × 2, 18 H, OMe, *J*(PH) 12], 7.10, 7.22 [$(AB)_2$, 4 H, C_6H_4, *J*(AB) 8]	[g] 271.2 [d, μ-C, *J*(PC) 45], 231.5, 222.8 (WCO), 174.0 [t, IrCO, *J*(PC) 8], 157.8 [$C^1(C_6H_4)$], 136.1, 129.0, 127.5 (C_6H_4), 61.8, 60.1 (*C*Me), 53.9, 53.3 [d × 2, OMe, *J*(PC) 5], 36.9, 30.4 (C*Me*), 21.4 (Me-4)
(8)		[h] −8.1 [q br, 1 H, IrH, *J*(PH) 20], 1.27 (m, 18 H, MeP), 1.83 (m, 9 H, MeP), 2.17 (s, 9 H, CMe and Me-4), 7.10, 8.08 [$(AB)_2$, 4 H, C_6H_4, *J*(AB) 8]	[g] 296.5 (m, μ-C), 228.5 (WCO), 152.8 [$C^1(C_6H_4)$], 140.4, 135.5, 130.7 (C_6H_4), 57.1 (br, *C*Me), 30.7 (C*Me*), 24.4—21.2 (MeP and Me-4)
(9)[d]	A	−11.52 [d of d, 1 H, HIr, *J*(PH) 13, 17], 2.11, 2.13, 2.17 (s × 3, 9 H, CMe and Me-4), 2.80—3.00 (m br, 4 H, CH_2), 6.42, 6.48 [$(AB)_2$, 4 H, C_6H_4, *J*(AB) 8], 6.60—8.00 (m, 20 H, Ph)	271.0 [d, μ-C, *J*(PC) 28], 228.7, 225.5 (WCO), 175.7 (IrCO), 156.5 [$C^1(C_6H_4)$], 135.1—121.8 (C_6H_4 and Ph), 60.2, 59.7 (*C*Me), 36.6 [d of d, CH_2, *J*(PC) 37, 15], 32.6 [d of d, CH_2, *J*(PC) 43, 9], 30.7, 29.8 (C*Me*), 21.2 (Me-4)
	B	−12.09 [d of d, 1 H, HIr, *J*(PH) 12, 18], 2.06 2.07, 2.10 (s × 3, 9 H, CMe and Me-4), 2.20—2.60 (m br, 4 H, CH_2), 6.36, 6.42 [$(AB)_2$, 4 H, C_6H_4, *J*(AB) 8], 6.60—8.00 (m, 20 H, Ph)	267.4 [d, μ-C, *J*(PC) 30], 228.5, 220.4 (WCO), 175.1 (IrCO), 156.0 [d, $C^1(C_6H_4)$, *J*(PC) 5], 135.1—121.8 (C_6H_4 and Ph), 63.2, 60.1 (*C*Me), 36.1 (C*Me*), 33.8 [d of d, CH_2, *J*(PC) 39, 15], 32.4 [d of d, CH_2, *J*(PC) 34, 7], 30.4 (C*Me*), 21.2 (Me-4)
(10)[d]	A	−21.3 (s, 1 H, HIr), 2.12, 2.15, 2.56 (s × 3, 9 H, CMe and Me-4), 5.74, 6.49 [$(AB)_2$, 4 H, C_6H_4, *J*(AB) 8], 7.32—7.48 (m, 2 H, bipy), 7.67—7.92 (m, 4 H, bipy), 8.83—9.01 (m, 2 H, bipy)	[g] 278.2 [μ-C, *J*(WC) 127], 228.7 [WCO, *J*(WC) 172], 222.2 [WCO, *J*(WC) 168], 175.6 (IrCO), 156.6—123.6 (C_6H_4 and bipy), 63.4, 62.6 (*C*Me), 36.9, 29.8 (C*Me*), 21.2 (Me-4)
	B	−22.6 (s, 1 H, HIr), 2.12, 2.20, 2.25 (s × 3, 9 H, CMe and Me-4)	284.3 (μ-C), 226.1, 225.6 (WCO), 178.0 (IrCO)
(11)		−15.28 [d of d of d, 1 H, HIr, *J*(PH) 130, 23, 12], 0.96 [d, 9 H, MeP, *J*(PH) 8], 1.59 [d, 18 H, MeP, *J*(PH) 7], 1.72 [d, 9 H, MeP, *J*(PH) 9], 2.19, 2.26, 2.47 (s × 3, 9 H, CMe and Me-4), 3.73 [d, 1 H, C(H)Ir, *J*(PH) 4], 6.88, 7.49 [$(AB)_2$, 4 H, C_6H_4, *J*(AB) 8]	244.2 [d, CO, *J*(PC) 10], 243.2 [d, CO, *J*(PC) 10], 147.2 [d, $C^1(C_6H_4)$, *J*(PC) 5], 135.1, 129.4, 128.9 (C_6H_4), 80.2 [br, C(H)B], 67.1 (*C*Me), 37.2, 32.6 (C*Me*), 26.5 (MeP), 23.3 [d, MeP, *J*(PC) 24], 22.9 [d, MeP, *J*(PC) 24], 21.5 (Me-4), 15.0 [d, MeP, *J*(PC) 29]
(12)		−13.82 [d of d, 1 H, HIr, *J*(PH) 21, 20], 2.17, 2.21, 2.40 (s × 3, 9 H, CMe and Me-4), 3.31 [d, 9 H, OMe, *J*(PH) 10], 3.55—3.65 (m, 27 H, OMe), 4.70 [br, 1 H, C(H)Ir], 6.92, 7.50 [$(AB)_2$, 4 H, *J*(AB) 8]	[f] 239.7 [d, WCO, *J*(PC) 15], 228.4 [d of d, WCO, *J*(PC) 12, 13], 146.9 [d, $C^1(C_6H_4)$, *J*(PC) 5], 135.1, 129.9, 128.5, 127.9 (C_6H_4), 91.4 (br, CHIr), 69.1 (br, *C*Me), 63.6 (*C*Me), 53.3 [d, OMe, *J*(PC) 7], 36.0 [d, C*Me*, *J*(PC) 3], 30.4 (C*Me*), 21.6 (Me-4)

[a] Chemical shifts are in p.p.m., coupling constants in Hz, measurements at room temperature unless otherwise stated. [b] Measured in CD_2Cl_2 unless otherwise stated. [c] Hydrogen-1 decoupled, chemical shifts are positive to high frequency of $SiMe_4$. Measurements are in CD_2Cl_2—CH_2Cl_2 unless otherwise stated. [d] Isomers, see text. [e] In C_6D_6. [f] Measured at −60 °C. [g] In thf–C_6D_6 (10:1). [h] In $CDCl_3$.

the isomers (**3a**) and (**3b**) on the n.m.r. time-scale. This would explain the appearance of four terminal CO stretches in the i.r. spectrum when measured in light petroleum. However, if there is an exchange between (**3a**) and (**3b**) it must proceed with an exceedingly low activation energy since spectra measured at low temperatures, down to −100 °C in $C_6D_5CD_3$ for $^{31}P-\{^1H\}$, did not display extra signals.

The two structures (**3a**) and (**3b**) differ only as to which BH group in the η^5-C_2B_3 face of the cage is involved in B–H→Ir bonding. The recently reported compound [$WRu(\mu\text{-}CC_6H_3Me_2\text{-}2,6)(CO)_3(\eta\text{-}C_5H_5)(\eta^5\text{-}C_2B_9H_9Me_2)$] appears to show isomerism of this kind, although one isomer, corresponding to the less symmetrical structure (**3b**), predominates.[5a] Moreover, in the room-temperature $^{13}C-\{^1H\}$ n.m.r. spectrum of the tungsten–ruthenium species peaks due to two isomers (9:1) are observed, so that exchange between the tautomers requires more energy than for (**3**), if it occurs in the latter species. It is possible that the i.r. spectrum of (**3**) in the CO stretching region in light petroleum solutions may be explained, not by the presence of (**3b**), but by the ability of (**3a**) to exist in two slightly different conformations. These conformers might be insufficiently different to display two discrete sets of n.m.r. signals even at low temperatures but distinct enough to effect the i.r. spectrum under highly resolving conditions.

The $^{13}C-\{^1H\}$ and $^{31}P-\{^1H\}$ n.m.r. data (Tables 2 and 3) when measured in CD_2Cl_2 clearly revealed the presence of more than one isomer. From relative peak intensities it was evident that the dominant species (2:1) was the one observed in C_6D_6

solutions, *i.e.* (**3a**), or a mixture of the latter with (**3b**). We assign the second isomer structure (**3c**), analogous to those of (**1a**) and (**1c**).[3] In the ^{31}P-$\{^1H\}$ n.m.r. spectrum of the isomeric mixture, measured in CD_2Cl_2 at room temperature, there are two peaks at δ 20.8 and 22.3 p.p.m., corresponding to (**3a**) and (**3c**), respectively. On cooling to −100 °C the signal due to (**3a**) remains a singlet whereas the peak due to (**3c**) in the room-temperature spectrum is replaced by two very broad resonances at δ 23.1 and 26.3 p.p.m. Evidently a dynamic process which equivalences the two phosphine environments is occurring. Two fluxional pathways which could achieve this have been discussed previously for (**1a**) and (**1c**).[3] For (**3c**) the lowest-energy process is probably a rotation or partial rotation of the $W(CO)_2(\eta^5\text{-}C_2B_9H_9Me_2)$ group about an axis through the midpoint of the Ir–μ-C bond, *via* an intermediate in which two semi-bridging carbonyls are present. The second process, in which the $Ir(PEt_3)_2$ fragment rotates about its C_2 axis, is likely to be of higher energy, and is not necessary to explain the n.m.r. data for (**3c**).

The i.r. and n.m.r. data for (**2**) indicated the existence of two isomers (**2a**) and (**2c**). However, in contrast with (**3**), the species (**2c**), in which the carbaborane group plays a spectator role, is also present in C_6D_6 solutions [(**2a**):(**2c**) 5:1], as well as being the dominant isomer in $CDCl_3$ or CD_2Cl_2 solutions [(**2a**):(**2c**) 1:2]. Although, as with (**3**), the relative proportions of the isomers show little change with temperature, (**2c**) undergoes the dynamic exchange processes discussed earlier.[3] Thus in the ^{31}P-$\{^1H\}$ n.m.r. spectrum at room temperature there is one signal for this isomer (δ 30.3 p.p.m.), whereas at −95 °C there are two (δ 27.8 and 32.9 p.p.m.).

Irrespective of the solvent used (light petroleum, C_6H_6, or thf) the i.r. spectrum of (**4**) showed only two terminal CO stretches. The existence of a single isomer (**4a**) was confirmed by the n.m.r. data (Tables 2 and 3). In the ^1H n.m.r. spectrum the presence of the B–H→Ir group was established by the resonance at δ −2.1, and further confirmed by the ^{11}B-$\{^1H\}$ n.m.r. spectrum with a peak for a single boron nucleus at δ 29.4 p.p.m. The latter signal in a ^{11}B spectrum broadened its half-height width by *ca.* 60 Hz due to ^1H coupling.

The spectroscopic data for (**5**) provided no evidence for an isomer with structure (**5c**). The i.r. spectrum measured in thf showed only two terminal CO stretches (1 972 and 1 905 cm^{-1}), there being no band near 1 750 cm^{-1}. However the i.r. spectrum measured in light petroleum was similar to that of (**3**), revealing four terminal CO absorptions [1 978vs, 1 974s (sh), 1 914s, and 1 908s cm^{-1}]. Interpretation of the n.m.r. data presents the same problem as with (**3**). In both the ^1H and ^{11}B-$\{^1H\}$ spectra there is a peak due to a B–H→Ir fragment (Table 2). This may be due to a rapid equilibration between the two isomers (**5a**) and (**5b**) if the i.r. spectrum in light petroleum indicates the presence of two distinct but similar isomers. Alternatively, only (**5a**) may be

Table 3. Boron-11 and phosphorus-31 n.m.r. data[a] for the complexes

Compound	^{11}B[b](δ)	^{31}P[c](δ)
(**2**)[d]	−10.4 to −3.7 (BH), 30.2 (B–H–Ir) (**2a**)	[e]28.7 (br) (**2a**), 32.9 (br), 27.8 (br) (**2c**)
(**3**)[d]	[f]−10.0 to −7.0 (BH), 32.8 (B–H–Ir) (**3a**)	[e]25.3 (s) (**3a**), 26.3 (br), 23.1 (br) (**3c**)
(**4**)	[g]−8.3 (vbr, BH), 29.4 (B–H–Ir)	[e]81.9 (s)
(**5**)	−8.2 (vbr, BH), 31.2 (B–H–Ir)	[h]37.0 [d, PPh_3, *J*(PP) 39], 88.1 [d, $P(OMe)_3$, *J*(PP) 39]
(**6**)	−12.4 to −7.8 (BH), 30.7 (B–H–Ir)	[e]100.3 (s)
(**7**)	−18.3 to 5.1 (BH), 28.6 [d, BIr, *J*(PB) 98]	96.0 [d, *J*(PP) 24], 99.0 (vbr)
(**8**)[d]	[i]−20.4 to −2.2 (BH), 45.0 (BIr)	[i]−48.5 [t, *J*(PP) 21], −48.9 [d, *J*(PP) 21]
(**9**)[d]	−20.0 to 4.8 (BH), 29.1, 34.8 (BIr)	[j]22.2 (br), 27.0 [d, *J*(PP) 7] (isomer **B**); 27.7 (br), 38.7 [d, *J*(PP) 12] (isomer **A**)
(**10**)[d]	[i]−17.7 to 0.5 (BH), 23.2, (isomer **A**); 29.2 (BIr) (isomer **B**)	
(**11**)	[i]−18.2 to −4.4 (BH), 13.0 [BC(H)R], 34.3 [d, BIr, *J*(PB) 69]	[i]−66.1 [d of d, *J*(PP) 8, 26], −52.3 (vbr), −40.6 [d of t, *J*(PP) 8, 8, 16], −36.5 [d, of d, *J*(PP) 6, 16]
(**12**)	[i]−14.7 to −4.3 (BH), 14.0 [BC(H)R], 30.6 [d, BIr, *J*(PB) 98]	[i]102.7 [d of d, *J*(PP) 23, 32], 110.5 [d of d, *J*(PP), 23, 32], 113.7 (vbr), 124.3 [d of d, *J*(PP) 17,32, *J*(WP) 188]

[a] Chemical shifts in p.p.m., coupling constants in Hz, measurements in CD_2Cl_2 at ambient temperatures unless otherwise stated. [b] Hydrogen-1 decoupled, chemical shifts are positive to high frequency of BF_3·Et_2O (external). [c] Hydrogen-1 decoupled, chemical shifts are positive to high frequency of 85% H_3PO_4 (external). [d] Isomers, see text. [e] Measured at −95 °C. [f] Measured in $C_6D_5CD_3$. [g] Measured in C_6D_6. [h] Measured at −70 °C. [i] Measured in thf–C_6D_6 (10:1). [j] Measured at −80 °C.

Table 4. Selected internuclear distances (Å) and angles (°) for $[WIr(\mu\text{-}CC_6H_4Me\text{-}4)(CO)_2(PEt_3)_2(\eta^5\text{-}C_2B_9H_9Me_2)]$ (**3**) with estimated standard deviations in parentheses

W–Ir	2.590(1)	W–C(1)	2.45(1)	W–C(2)	2.44(1)	W–B(3)	2.37(1)
W–B(4)	2.32(1)	W–B(5)	2.42(2)	W–C(5)	1.97(1)	W–C(6)	1.96(1)
W–C(10)	2.06(1)	Ir–P(1)	2.258(3)	Ir–P(2)	2.257(3)	Ir–B(4)	2.34(1)
Ir–C(10)	1.95(1)	C(1)–C(2)	1.60(2)	C(1)–C(3)	1.55(2)	C(1)–B(5)	1.71(2)
C(1)–B(6)	1.72(2)	C(1)–B(10)	1.74(2)	C(2)–C(4)	1.56(2)	C(2)–B(3)	1.70(2)
C(2)–B(6)	1.74(2)	C(2)–B(7)	1.70(2)	B(3)–B(4)	1.83(2)	B(3)–B(7)	1.80(2)
B(3)–B(8)	1.79(2)	B(4)–B(5)	1.84(2)	B(4)–B(8)	1.78(2)	B(4)–B(9)	1.79(2)
B(5)–B(9)	1.75(2)	B(5)–B(10)	1.74(2)	B(6)–B(7)	1.73(2)	B(6)–B(10)	1.75(2)
B(6)–B(11)	1.73(2)	B(7)–B(8)	1.81(2)	B(7)–B(11)	1.74(2)	B(8)–B(9)	1.78(2)
B(8)–B(11)	1.82(2)	B(9)–B(10)	1.76(2)	B(9)–B(11)	1.80(2)	B(10)–B(11)	1.76(2)
C(5)–O(5)	1.15(2)	C(6)–O(6)	1.18(2)	C(10)–C(11)	1.44(2)	Ir–H(4)	1.80*
Ir–W–B(4)	56.5(2)	Ir–W–C(5)	112.8(4)	Ir–W–C(6)	117.0(4)	C(5)–W–C(6)	88.1(6)
Ir–W–C(10)	48.0(3)	C(5)–W–C(10)	81.1(5)	C(6)–W–C(10)	81.6(5)	W–Ir–P(1)	131.7(1)
W–Ir–P(2)	132.4(1)	P(1)–Ir–P(2)	95.7(1)	W–Ir–B(4)	55.9(2)	W–Ir–C(10)	51.6(3)
P(1)–Ir–C(10)	112.8(3)	P(2)–Ir–C(10)	112.0(3)	W–B(4)–Ir	67.5(3)	Ir–H(4)–B(4)	100*
W–C(5)–O(5)	172.6(12)	W–C(6)–O(6)	174.2(12)	W–C(10)–Ir	80.4(4)	W–C(10)–C(11)	140.3(7)
Ir–C(10)–C(11)	139.3(7)						

* H(4) Located from a low-angle difference map, co-ordinates not refined.

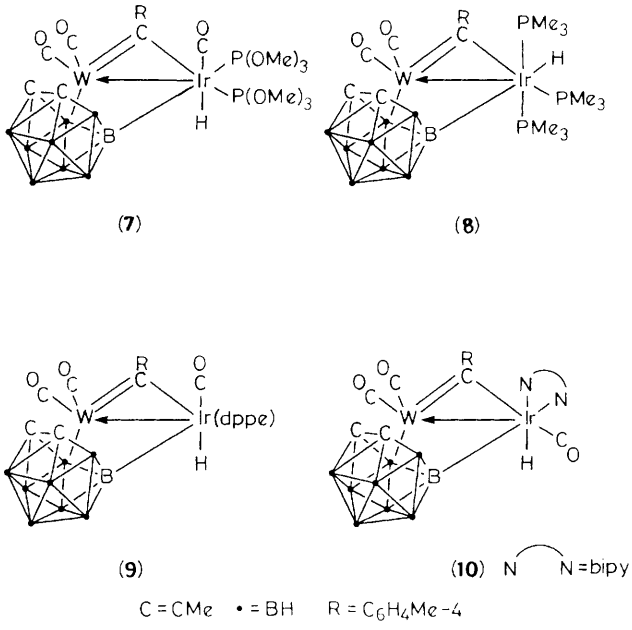

present, if the i.r. data reflect a subtle structural change in the single isomer allowing two conformers to exist.

The presence of the $Ir(PPh_3)\{P(OMe)_3\}$ fragment in (**5**) introduces an asymmetry not present in the other complexes. The $^{31}P-\{^1H\}$ n.m.r. spectrum, therefore, shows two resonances, each a doublet, at δ 37.0 and 88.1 p.p.m. [*J*(PP) 39 Hz]. The CMe groups in the carbaborane cage are no longer related by a plane of symmetry and so there are two *C*Me resonances (63.0 and 63.5 p.p.m.). However, the asymmetry introduced at the iridium centre is insufficient to affect the C*Me* groups which therefore give a single peak (32.0 p.p.m.).

The spectroscopic data for (**6**), like that of (**4**), were relatively simple in accord with there being only one isomer (**6a**). In all solvents, including light petroleum, there were only two terminal CO bands. The ^1H and $^{11}B-\{^1H\}$ n.m.r. spectra each showed a resonance confirming the presence of the B–H→Ir fragment.

As described above, the isomer ratios for the species $[WIr(\mu\text{-}CC_6H_4Me\text{-}4)(CO)_2L_2(\eta^5\text{-}C_2B_9H_9Me_2)]$ [*e.g.* (**3a**):(**3c**)] are dependent on both the solvent and the ligand L. It is possible to provide a tentative explanation for these trends by considering the likely distribution of charge in these species. The formation of a neutral W–Ir complex from the fragments $[W(\equiv CC_6H_4Me\text{-}4)(CO)_2(\eta^5\text{-}C_2B_9H_9Me_2)]^-$ and IrL_2^+ probably affords a complex product in which some residual positive charge remains at the iridium centre, which can formally be considered as Ir^I, the carbaborane cage carrying some negative charge. The formation of the B–H→Ir bond would then provide a mechanism for the stabilisation of these charges. Such an interaction would be most important when the ligands attached to iridium are unable to stabilise a positive charge at the iridium centre by electron donation. The phosphite ligands $P(OMe)_3$ and $P(OPh)_3$ are poorer electron donors than the phosphines PPh_3 and PEt_3. This may explain why the isomers (**4c**) and (**6c**), with phosphite ligands but no stabilising B–H→Ir interactions, are not observed.

The co-ordination of the B–H bond to iridium is also expected to lead to a reduction in the molecular dipole moment. This might arise as a result of the electron-donor properties of the B–H bond, and because the carbaborane cage and iridium centre are physically closer together, rather than being at opposite ends of the molecule, as they are for isomers (**2c**)—(**6c**). This would explain the fact that the isomers (**2c**) and (**3c**), which will be more polar, are only observed in the most polar solvents.

The isolation of species containing three-centre two-electron B–H→Ir bonds contrasts with the earlier studies involving rhodium which produced compounds of type (**1**), in which the carbaborane group ligates the tungsten centre only. The greater reactivity of the iridium system was further demonstrated by the synthesis of compounds with Ir–H and B–Ir σ bonds. These products evidently form *via* intermediates having B–H→Ir groups. Thus in the synthesis of (**6**) a small amount of the compound $[WIrH(\mu\text{-}CC_6H_4Me\text{-}4)(\mu\text{-}\sigma\text{:}\eta^5\text{-}C_2B_9H_8Me_2)(CO)_3\{P(OMe)_3\}_2]$ (**7**) was obtained, together with a trace of another product discussed below. Compound (**7**) could be prepared in better yield (*ca.* 50%) by treating thf solutions of (**6**) with CO for a few seconds. Longer treatment leads to decomposition. Complex (**7**) was characterised by the data given in Tables 1—3. Interestingly, solutions of (**7**) release CO on standing, a process which produces its precursor (**6**), together with unidentified products. We have previously observed that the compound $[WPt(\mu\text{-}CC_6H_3Me_2\text{-}2,6)(\mu\text{-}\sigma\text{:}\eta^5\text{-}C_2B_9H_8Me_2)(CO)_2(PEt_3)]$ which contains an exopolyhedral B–Pt σ bond reacts reversibly with hydrogen to give $[WPtH(\mu\text{-}CC_6H_3Me_2\text{-}2,6)(CO)_2(PEt_3)(\eta^5\text{-}C_2B_9H_9Me_2)]$, a species having a B–H→Pt fragment.[2]

The spectroscopic properties of (**7**) were in accord with the structure proposed. The i.r. spectrum showed three terminal CO stretches, and a weak absorption at 2 140 cm^{-1} is ascribed to the Ir–H group. The presence of the latter was confirmed by the ^1H n.m.r. spectrum which showed a high field resonance (doublet of doublets) at δ −12.52 [*J*(PH) 18 and 9 Hz]. The $^{13}C-\{^1H\}$ n.m.r. spectrum was also informative. As with other compounds reported herein, there was a characteristic resonance for the alkylidyne-carbon nucleus. For (**7**) this signal was a doublet at δ 271.2 p.p.m. due to coupling (45 Hz) with the transoid $^{31}P(OMe)_3$ nucleus. In the carbonyl region there were three resonances, due to the $W(CO)_2$ (δ 231.5 and 222.8 p.p.m.) and IrCO moieties [δ 174.0 p.p.m., t, *J*(PC) 8 Hz]. The triplet pattern for the latter signal indicates a *cis*-$Ir\{P(OMe)_3\}_2$ arrangement. Moreover, in a ^{13}C n.m.r. spectrum the IrCO resonance became a doublet of triplets [*J*(HC) 47, *J*(PC) 8 Hz], as a result of the *trans*-$^1HIr^{13}CO$ coupling. The $^{31}P-\{^1H\}$ n.m.r. spectrum consisted of two signals at δ 96.0 and 99.0 p.p.m. The former was a doublet, the magnitude (24 Hz) of the $^{31}P-^{31}P$ coupling being as expected for a *cis*-$Ir\{P(OMe)_3\}_2$ group. The peak at 99.0 p.p.m. was very broad, and we assign this to the ^{31}P nucleus transoid to the B–Ir σ bond. The presence of the latter was confirmed by the $^{11}B-\{^1H\}$ n.m.r. spectrum which showed a doublet resonance corresponding to one boron nucleus at δ 28.6 p.p.m. [*J*(PB) 98 Hz]. The other boron peaks were in the range δ −18.3 to 5.1 p.p.m. In the compound $[WPt(\mu\text{-}CC_6H_3Me_2\text{-}2,6)(\mu\text{-}\sigma\text{:}\eta^5\text{-}C_2B_9H_8Me_2)(CO)_2(PEt_3)]$, for which two isomers with B–Pt bonds have been identified, these groups give ^{11}B n.m.r. resonances at δ 24.7 and 29.2 p.p.m.[2] The latter peak corresponds to the isomer in which it is the central boron CCB*B*B of the η^5 face of the cage which is σ bonded to platinum and is thus analogous to the structural arrangement proposed for (**7**).

The reaction between PMe_3 and (**2**) did not afford a product akin to the complexes (**3**)—(**6**), although such a species may well be an intermediate. An oxidative-addition process occurred at the iridium centre to yield the complex $[WIrH(\mu\text{-}CC_6H_4Me\text{-}4)(\mu\text{-}\sigma\text{:}\eta^5\text{-}C_2B_9H_8Me_2)(CO)_2(PMe_3)_3]$ (**8**). Unfortunately microanalytically pure samples of this product could not be obtained, and the species appeared to exist in thf solutions as a major and a minor isomer (5:1). In thf there are three terminal CO stretches (Table 1), whereas the structure depicted for (**8**) would be expected to reveal two such bands. The n.m.r. signals for the main isomer, however, are in good

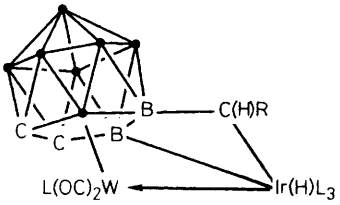

C = CMe • = BH R = C_6H_4Me-4

L

(11) PMe_3

(12) $P(OMe)_3$

agreement with the structure shown. The ^1H n.m.r. spectrum has a resonance for the IrH group at δ −8.1, and the ^{11}B-{^1H} n.m.r. spectrum has a diagnostic peak for the IrB moiety at δ 45.0 p.p.m. At room temperature the ^{31}P-{^1H} n.m.r. spectrum consists of a single peak, but at −80 °C resonances are observed at δ −48.5 [t, 1 P, J(PP) 21] and −48.9 p.p.m. [d, 2 P, J(PP) 21 Hz].

Reactions between the salts $[IrL_2(cod)][PF_6]$ [L_2 = dppe ($Ph_2PCH_2CH_2PPh_2$) or bipy (2,2′-bipyridine)] and $[N(PPh_3)_2][W(\equiv CC_6H_4Me\text{-}4)(CO)_2(\eta^5\text{-}C_2B_9H_9Me_2)]$ afforded, respectively, the products $[WIrH(\mu\text{-}CC_6H_4Me\text{-}4)(\mu\text{-}\sigma\text{:}\eta^5\text{-}C_2B_9H_8Me_2)(CO)_3(dppe)]$ (**9**) and $[WIrH(\mu\text{-}CC_6H_4Me\text{-}4)(\mu\text{-}\sigma\text{:}\eta^5\text{-}C_2B_9H_8Me_2)(CO)_3(bipy)]$ (**10**) which contained IrH and B–Ir groups. Data for these species are given in Tables 1—3. Interestingly, the corresponding reaction between [Rh(dppe)(cod)][PF_6] and $[N(PPh_3)_2][W(\equiv CR)(CO)_2(\eta\text{-}C_5H_5)]$ gave compound (**1b**) in which the carbaborane ligand adopts a spectator role.

Both (**9**) and (**10**) exist as mixture of two isomers **A** and **B** in toluene, CD_2Cl_2, or thf solutions. Thus the i.r. spectra (Table 1), irrespective of the solvent used, show four terminal CO stretches rather than the three anticipated for a single isomer. Examination of the ^{11}B-{^1H} n.m.r. spectra revealed that for each isomer of either (**9**) or (**10**) there is a diagnostic peak for a B–Ir group (Table 3). In the ^1H n.m.r. spectra of (**9**) and (**10**) there are two high-field signals due to terminal Ir–H groups, again showing the presence of two isomers for each species. The isomerism may well relate to which boron atom in the η^5-C_2B_3 face of the cage forms the σ bond to the iridium. This boron atom may be the central one in the $\overline{CCBBB}$ ring, as in the structural formulae for (**9**) and (**10**) depicted, or it may be a boron atom adjacent to carbon in the $\overline{CCBBB}$ ring. Examination of peak intensities in the n.m.r. spectra showed that the proportions of the isomers varied with the solvent. The exchange between B–Ir sites would be readily explicable in terms of intermediates containing B–H→Ir groups formed by migration of the terminal hydrido ligand to a bridging position *i.e.* reformation of what are very likely the precursors to (**9**) and (**10**). A temporary rupture of the three-centre bond with rotation of the η^5-$C_2B_9H_9Me_2$ ligand would provide a pathway for formation of a new B–H→Ir linkage from a different boron atom, as postulated previously in the isomerism of related tungsten–platinum compounds.[2]

The *trans*-IrH(CO) arrangement present in the two isomers of (**9**) was established from ^{13}C n.m.r. measurements. The iridium-ligated CO resonance for each isomer was a doublet with J(CH) 46 Hz. In contrast, the IrCO resonances in the coupled ^{13}C n.m.r. spectra of the isomers of (**10**) remained as singlets as expected for a *cis*-IrH(CO) fragment. This was supported by the chemical shifts observed at high field for the IrH group in the ^1H n.m.r. spectrum of each isomer (Table 2). The chemical shifts (δ −21.3 and −22.6) are in the region established for a hydrido-iridium complex in which a nitrogen donor ligand occupies the *trans* position.[18]

During the course of the work described in this paper we also isolated the novel compounds $[WIrH\{\mu\text{-}\sigma\text{:}\eta^5\text{-}CH(C_6H_4Me\text{-}4)(C_2B_9H_7Me_2)\}(CO)_2(PR_3)_4]$ [R = Me (**11**) or OMe (**12**)]. It was mentioned earlier that in the synthesis of (**6**) small amounts of (**7**) and another product were obtained. The latter proved to be (**12**) which could be prepared in yields of *ca.* 40% by treatment of complex (**2**) with a ten-fold excess of $P(OMe)_3$. Similarly, the reaction between (**2**) and an excess of PMe_3 in thf after several hours gave (**11**).

The compounds (**11**) and (**12**) contain a B–$CH(C_6H_4Me\text{-}4)$–Ir group which would form *via* insertion of a *p*-tolylmethylidyne ligand into a B–H→Ir unit of the type present in (**6a**). However, (**11**) and (**12**) also contain B–Ir and IrH groups as do (**7**) or (**8**), and so intermediates with these structural features are implicated. Whatever the pathways leading to (**11**) and (**12**), as mentioned in the Introduction, dimetal W–Mo and W–Ru complexes are known having related B–$CH(C_6H_4Me\text{-}4)$–M (Mo or Ru) bridge systems.[4a,b] Moreover, the reaction between $[NEt_4][Mo(\equiv CC_6H_4Me\text{-}4)(CO)\{P(OMe)_3\}(\eta^5\text{-}C_2B_9H_9Me_2)]$ and $[Fe_2(CO)_9]$ yields the mononuclear metal complex $[NEt_4][Mo\{\sigma,\eta^5\text{-}CH(C_6H_4Me\text{-}4)(C_2B_9H_8Me_2)\}(CO)_3]$ in which a B–$CH(C_6H_4Me\text{-}4)$–Mo group is present.[19]

The n.m.r. data (Tables 2 and 3) for (**11**) and (**12**) are in accord with the structures proposed, but only that of (**12**) is discussed. The ^1H n.m.r. spectrum shows a resonance for the hydrido ligand attached to the iridium at δ −13.82, the signal appearing as a doublet of doublets [J(PH) 21, 201 Hz]. A broad peak at δ 4.70 corresponding to one proton is assigned to the IrCH group. In the spectrum of $[MoW\{\mu\text{-}\sigma\text{:}\eta^3\text{-}CH(C_6H_4Me\text{-}4)(C_2B_9H_8Me_2)\}(CO)_3(\eta\text{-}EtC_2Et)(\eta^5\text{-}C_9H_7)]$[6] the corresponding resonance is at δ 5.01. In the ^{13}C-{^1H} n.m.r. spectrum of (**12**) the peak at δ 91.4 p.p.m. is assigned to the C(H)Ir nucleus. In a ^{13}C n.m.r. spectrum this signal became a doublet [J(HC) 30 Hz], confirming the assignment. The ^{11}B-{^1H} n.m.r. spectrum shows resonances at δ 14.0 (BCH) and 30.6 p.p.m. (BIr), the latter being a doublet [J(PB) 98 Hz]. Again the signals agree closely with those observed for other compounds showing similar structural features.[2,4,6] The ^{31}P-{^1H} n.m.r. spectrum, as expected, showed four resonances: δ 102.7 [d of d, J(PP) 23, 32], 110.5 [d of d, J(PP) 23, 32], 113.7 (vbr), and 124.3 p.p.m. [d of d, J(PP) 17, 32, J(WP) 188 Hz].

The results reported in this paper show that the chemistry of the tungsten–iridium compounds is very different from that of the previously reported [3] tungsten–rhodium complexes. Most of the new compounds described herein have no structural counterparts in the tungsten–rhodium system. There is clearly a marked propensity of iridium, compared with rhodium, to form exopolyhedral bonds with the carbaborane cage.

Experimental

Experiments were carried out using Schlenk-tube techniques, under a dry oxygen-free nitrogen atmosphere. Light petroleum refers to that fraction of b.p. 40—60 °C. Chromatography columns were of alumina (Brockman Activity II) or Florisil (Aldrich, 100—200 mesh). The compounds $[N(PPh_3)_2][W(\equiv CC_6H_4Me\text{-}4)(CO)_2(\eta^5\text{-}C_2B_9H_9Me_2)]$,[3] $[Ir(PPh_3)_2(cod)][PF_6]$,[20] $[IrL_2(cod)][PF_6]$ (L_2 = dppe[20] or bipy[21]) were prepared by methods previously described. Analytical and other data for the new compounds are given in Table 1. The n.m.r. measurements were made with JEOL JNM FX90Q, GX270, and GX400 spectrometers. The i.r. spectra were recorded with Nicolet 10-MX and 5Z-DX spectrophotometers.

Preparation of the Compound $[WIr(\mu\text{-}CC_6H_4Me\text{-}4)(CO)_2(PPh_3)_2(\eta^5\text{-}C_2B_9H_9Me_2)]$.—A mixture of $[N(PPh_3)_2]$-

$[W(\equiv CC_6H_4Me\text{-}4)(CO)_2(\eta^5\text{-}C_2B_9H_9Me_2)]$ (0.54 g, 0.52 mmol) and $[Ir(PPh_3)_2(cod)][PF_6]$ (0.50 g, 0.52 mmol) was stirred in thf (30 cm^3) for 1 h at room temperature, thereby affording a green-black solution. Solvent was removed *in vacuo*, and the residue was extracted first with thf–light petroleum (10 × 10 cm^3, 1:1) and then with the same solvents (10 × 10 cm^3, 2:1). The extracts were chromatographed on an alumina column (3 × 20 cm). Elution with thf–light petroleum (2:1) removed a broad green band. Removal of solvent *in vacuo* gave black-green *microcrystals* of $[WIr(\mu\text{-}CC_6H_4Me\text{-}4)(CO)_2(PPh_3)_2(\eta^5\text{-}C_2B_9H_9Me_2)]$ (**2**) (0.49 g).

Reactions of $[WIr(\mu\text{-}CC_6H_4Me\text{-}4)(CO)_2(PPh_3)_2(\eta^5\text{-}C_2B_9H_9Me_2)]$ *with Donor Ligands.*—In these syntheses compound (**2**) was prepared *in situ* by mixing equivalent amounts of $[Ir(PPh_3)_2(cod)][PF_6]$ and $[N(PPh_3)_2][W(\equiv CC_6H_4Me\text{-}4)(CO)_2(\eta^5\text{-}C_2B_9H_9Me_2)]$ in thf, and the resulting solution was treated with the appropriate donor ligand to displace the PPh_3 groups.

(*i*) Complex (**2**) (0.38 mmol) in thf (25 cm^3) was treated with PEt_3 (0.69 cm^3, 5.76 mmol), and the mixture was stirred at room temperature for 1.5 h. The dark red solution was reduced in volume *in vacuo* to *ca.* 5 cm^3, and chromatographed on Florisil (2 × 20 cm column). Elution with light petroleum (*ca.* 150 cm^3) and with thf–light petroleum (*ca.* 50 cm^3, 1:4) removed cod, PPh_3, excess of PEt_3, and a trace of an unidentified yellow material. Subsequent elution with thf–light petroleum (1:1) gave a brown fraction. Removal of solvent *in vacuo* gave red-brown *microcrystals* of $[WIr(\mu\text{-}CC_6H_4Me\text{-}4)(CO)_2(PEt_3)_2(\eta^5\text{-}C_2B_9H_9Me_2)]$ (**3**) (0.30 g).

(*ii*) Similarly, complex (**2**) (0.30 mmol) in thf (15 cm^3) was treated with $P(OPh)_3$ (1.6 cm^3, *ca.* 6 mmol), and the mixture was stirred for 8 h. After reducing the solvent *in vacuo* to *ca.* 5 cm^3, the solution was chromatographed on alumina (2 × 40 cm column). Treatment of the alumina with light petroleum (*ca.* 200 cm^3) removed impurities. Elution with Et_2O–light petroleum (1:2) afforded a yellow-green band, which after removal of solvent from the eluate *in vacuo* gave an oily product. The latter was dissolved in the minimum of Et_2O and rechromatographed using Florisil (2 × 20 cm column at −20 °C). After washing the column with light petroleum (*ca.* 200 cm^3), a broad yellow-green band was eluted with Et_2O–light petroleum (1:4). Removal of solvent *in vacuo* yielded yellow-green *microcrystals* of $[WIr(\mu\text{-}CC_6H_4Me\text{-}4)(CO)_2\{P(OPh)_3\}_2(\eta^5\text{-}C_2B_9H_9Me_2)]$ (**4**) (0.14 g).

(*iii*) (*a*) A sample of $P(OMe)_3$ (30 μl, 0.25 mmol) was added to complex (**2**) (0.15 mmol) in thf (10 cm^3), and the mixture was stirred for 20 h. Solvent was removed *in vacuo*, and the residue was suspended in thf (3 cm^3) and placed on a Florisil column (2 × 30 cm). After washing the column with light petroleum (*ca.* 100 cm^3) to remove excess of $P(OMe)_3$, PPh_3, and cod, elution was continued with thf–light petroleum (1:4) thereby giving an orange fraction, followed by an orange-brown product. The first fraction contained a small amount of (**6**). The second fraction, after removal of solvent *in vacuo*, gave orange-brown *microcrystals* of $[WIr(\mu\text{-}CC_6H_4Me\text{-}4)(CO)_2(PPh_3)\{P(OMe)_3\}(\eta^5\text{-}C_2B_9H_9Me_2)]$ (**5**) (0.075 g). A small amount (15 mg) of (**2**) was recovered from the column by elution with thf–light petroleum (1:1).

(*b*) Similarly, $P(OMe)_3$ (60 μl, 0.51 mmol) and complex (**2**) (0.20 mmol) in thf (30 cm^3) after 24 h stirring gave orange *microcrystals* of $[WIr(\mu\text{-}CC_6H_4Me\text{-}4)(CO)_2\{P(OMe)_3\}_2(\eta^5\text{-}C_2B_9H_9Me_2)]$ (**6**) (0.085 g), after chromatography on Florisil, eluting with thf–light petroleum (1:4), and removal of solvent. Trace amounts of (**7**) and (**12**) were recovered and identified by i.r. spectroscopy.

(*c*) A sample of complex (**2**) (0.20 mmol) in thf (30 cm^3) was treated with $P(OMe)_3$ (60 μl, 0.51 mmol), and the mixture was stirred for 24 h. Carbon monoxide was then gently bubbled into the solution for *ca.* 30 s, and stirring was continued for 10 min. Solvent was removed *in vacuo*, and the residue was dissolved in thf (30 cm^3) and chromatographed on a Florisil column (2 × 30 cm). After washing the column with light petroleum (100 cm^3), elution with thf–light petroleum (1:2) led to the recovery of a trace of (**12**) (*ca.* 15 mg). Further elution with the same solvents (1:1) yielded a trace of (**5**) and (**6**). Finally, elution with thf–light petroleum (3:1) yielded a brown fraction, which after removal of solvent *in vacuo* gave yellow-brown *microcrystals* of $[WIrH(\mu\text{-}CC_6H_4Me\text{-}4)(\mu\text{-}\sigma\text{:}\eta^5\text{-}C_2B_9H_8Me_2)(CO)_3\{P(OMe)_3\}_2]$ (**7**) (0.09 g).

(*d*) The reagents (**2**) (0.20 mmol) and $P(OMe)_3$ (0.25 cm^3, 2.1 mmol) were stirred together in thf (15 cm^3) for 3 h. The solution was reduced *in vacuo* to *ca.* 5 cm^3, and chromatographed on a Florisil column (2 × 40 cm). After washing the column with light petroleum (*ca.* 100 cm^3) and thf–light petroleum (*ca.* 100 cm^3, 1:8), an orange band was eluted with the same solvents (1:2). After removal of solvent *in vacuo*, orange *microcrystals* of $[WIrH\{\mu\text{-}\sigma\text{:}\eta^5\text{-}CH(C_6H_4Me\text{-}4)(C_2B_9H_7Me_2)\}(CO)_2\{P(OMe)_3\}_4]$ (**12**) (0.10 g) were obtained.

(*iv*) (*a*) Compound (**2**) (0.20 mmol) in thf (20 cm^3) was treated with PMe_3 (0.1 cm^3, 1.0 mmol), and the mixture was stirred for 6 h. The volume was reduced *in vacuo* to *ca.* 5 cm^3, and the solution was chromatographed on Florisil (2 × 40 cm column). Elution with light petroleum (100 cm^3) removed displaced PPh_3 and cod. Further elution with thf–light petroleum (1:3) gave an orange eluate which afforded (**11**) (22 mg). Elution with the same solvents (1:2) removed a trace of unidentified yellow material. Final elution with thf–light petroleum (2:1) gave a green fraction which after removal of solvent *in vacuo* afforded green *microcrystals* of $[WIrH(\mu\text{-}CC_6H_4Me\text{-}4)(\mu\text{-}\sigma\text{:}\eta^5\text{-}C_2B_9H_8Me_2)(CO)_2(PMe_3)_3]$ (**8**) (0.095 g).

(*b*) An excess of PMe_3 (0.30 cm^3, 3.0 mmol) was added to complex (**2**) (0.15 mmol) in thf (10 cm^3), and the mixture was stirred for 48 h. Solvent was removed *in vacuo* and the orange-brown residue was suspended in a minimum of thf (*ca.* 3 cm^3) and chromatographed on Florisil (2 × 30 cm column). After washing the column with light petroleum, an orange-brown eluate was recovered by elution with thf–light petroleum (1:3). Removal of solvent *in vacuo* gave orange *microcrystals* of $[WIrH\{\mu\text{-}\sigma\text{:}\eta^5\text{-}CH(C_6H_4Me\text{-}4)(C_2B_9H_7Me_2)\}(CO)_2(PMe_3)_4]$ (**11**) (0.053 g). Small amounts of (**8**) were also recovered from the column.

Synthesis of the Complex $[WIrH(\mu\text{-}CC_6H_4Me\text{-}4)(\mu\text{-}\sigma\text{:}\eta^5\text{-}C_2B_9H_8Me_2)(CO)_3(dppe)]$.—A mixture of $[Ir(dppe)(cod)][PF_6]$ (0.50 g, 0.59 mmol) and $[N(PPh_3)_2][W(\equiv CC_6H_4Me\text{-}4)(CO)_2(\eta^5\text{-}C_2B_9H_9Me_2)]$ (0.62 g, 0.59 mmol) in thf (30 cm^3) was stirred at room temperature for 5 d. The resulting solution was reduced in volume *in vacuo* to *ca.* 5 cm^3, and chromatographed on an alumina column (2 × 25 cm). Elution with thf–light petroleum (2:1) gave an orange-brown eluate. Removal of solvent *in vacuo* gave orange-brown *microcrystals* of $[WIrH(\mu\text{-}CC_6H_4Me\text{-}4)(\mu\text{-}\sigma\text{:}\eta^5\text{-}C_2B_9H_8Me_2)(CO)_3(dppe)]$ (**9**) (0.35 g). Bubbling CO through the solution of the crude product before chromatography improves the yield.

Synthesis of the Complex $[WIrH(\mu\text{-}CC_6H_4Me\text{-}4)(\mu\text{-}\sigma\text{:}\eta^5\text{-}C_2B_9H_8Me_2)(CO)_3(bipy)]$.—A thf (20 cm^3) solution of $[Ir(bipy)(cod)][PF_6]$ (0.12 g, 0.20 mmol) and $[N(PPh_3)_2][W(\equiv CC_6H_4Me\text{-}4)(CO)_2(\eta^5\text{-}C_2B_9H_9Me_2)]$ (0.24 g, 0.20 mmol) was treated with a stream of CO for *ca.* 30 s, and the mixture was stirred for 1.5 h. After addition of light petroleum (5 cm^3) the solution was chromatographed on a Florisil column (3 × 15 cm). Elution with thf–light petroleum (4:1) gave a brown fraction, which after removal of solvent *in vacuo* afforded brown *microcrystals* of $[WIrH(\mu\text{-}CC_6H_4Me\text{-}4)(\mu\text{-}\sigma\text{:}\eta^5\text{-}C_2B_9H_8\text{-}$

Table 5. Atomic positional parameters (fractional co-ordinates $\times 10^4$) for compound (**3a**), with estimated standard deviations in parentheses

Atom	*x*	*y*	*z*
W	8 741(1)	7 723(1)	7 876(1)
Ir	7 418(1)	7 963(1)	7 534(1)
P(1)	6 769(1)	9 314(2)	7 308(2)
P(2)	6 508(1)	6 920(2)	7 508(2)
C(1)	9 681(5)	8 094(7)	6 696(9)
C(2)	9 564(5)	6 948(9)	6 731(9)
C(3)	10 301(6)	8 577(9)	7 256(11)
C(4)	10 072(6)	6 301(8)	7 355(10)
B(3)	8 719(7)	6 619(9)	6 517(10)
B(4)	8 259(4)	7 760(8)	6 282(9)
B(5)	8 929(6)	8 709(9)	6 405(11)
B(6)	9 988(7)	7 434(10)	5 697(10)
B(7)	9 385(7)	6 505(11)	5 569(11)
B(8)	8 541(7)	7 022(10)	5 267(10)
B(9)	8 678(6)	8 297(10)	5 218(10)
B(10)	9 564(7)	8 540(11)	5 486(11)
B(11)	9 355(7)	7 504(11)	4 772(10)
C(5)	8 929(7)	6 685(10)	8 853(9)
O(5)	8 974(7)	6 031(9)	9 384(9)
C(6)	9 186(7)	8 635(11)	8 804(11)
O(6)	9 400(6)	9 227(9)	9 367(9)
C(10)	7 904(5)	7 948(7)	8 819(9)
C(11)	7 750(5)	8 046(8)	9 868(8)
C(12)	7 048(6)	8 245(10)	10 159(9)
C(13)	6 858(6)	8 375(11)	11 171(9)
C(14)	7 360(6)	8 274(9)	11 917(9)
C(15)	8 043(5)	8 049(9)	11 639(8)
C(16)	8 214(5)	7 942(8)	10 638(8)
C(17)	7 170(8)	8 371(13)	13 009(8)
C(21)	7 376(5)	10 342(8)	7 147(10)
C(22)	7 802(7)	10 596(9)	8 055(11)
C(23)	6 200(6)	9 402(8)	6 208(7)
C(24)	6 568(7)	9 206(10)	5 239(9)
C(25)	6 207(6)	9 748(8)	8 330(9)
C(26)	5 818(7)	10 719(10)	8 109(10)
C(31)	6 790(7)	5 745(9)	8 019(9)
C(32)	6 937(9)	5 716(11)	9 122(11)
C(33)	5 714(6)	7 186(10)	8 199(11)
C(34)	5 164(8)	6 364(13)	8 270(14)
C(35)	6 151(6)	6 587(10)	6 273(10)
C(36)	6 659(7)	6 170(12)	5 532(11)

$Me_2)(CO)_3(bipy)]$ (**10**) (0.16 g). In the absence of CO, compound (**10**) is also obtained but more slowly, and in lower yield. If too much CO is added the product obtained is $[Ir(bipy)(CO)_3][PF_6]$.

Crystal-structure Determination of Compound (**3a**).—Black pyramidal crystals of complex (**3a**) were grown by solvent diffusion from thf–light petroleum. Diffracted intensities were collected at *ca.* 206 K from a crystal of dimensions *ca.* 0.40 × 0.45 × 0.45 mm on a Nicolet $P2_1$ diffractometer equipped with a modified Nicolet LT1 low-temperature attachment. Of the 4 517 unique data collected (ω—2θ scans, $2\theta \leqslant 55°$) 4 128 had $I \geqslant 2.5\sigma(I)$, and only these were used for structure solution and refinement. The data were corrected for Lorentz and polarisation effects and for *X*-ray absorption, the latter by an empirical method based on azimuthal scan data.[22]

Crystal data. $C_{26}H_{52}B_9IrO_2P_2W$, $M = 932.0$, orthorhombic, space group $P2_12_12$ (no. 18), $a = 19.109(7)$, $b = 13.782(3)$, $c = 13.367(5)$ Å, $U = 3\,520(2)$ Å^3 (at 206 K), $Z = 4$, $D_c = 1.76$ g cm^{-3}, $F(000) = 1\,799.5$, Mo-K_α *X*-radiation (graphite monochromator), $\bar{\lambda} = 0.710\,69$ Å, μ(Mo-K_α) = 72.1 cm^{-1}.

The structure was solved by conventional heavy-atom methods and successive difference Fourier syntheses were used to locate all non-hydrogen atoms, which were refined with anisotropic thermal parameters. The position of the hydrogen atom H(4) was determined from a low-angle difference ($2\theta \leqslant 35°$) map and was not refined. All remaining hydrogen atoms were included at calculated positions (C–H 0.96 Å and B–H 1.10 Å)[23] with common refined isotropic thermal parameters for chemically related methyl groups and fixed isotropic thermal parameters (*ca.* 1.2 × $U_{equiv.}$ of the parent carbon or boron atom) for all remaining hydrogen atoms. Refinement by blocked-cascade least squares led to $R = 0.037$ ($R' = 0.037$), with a weighting scheme of the form $w^{-1} = [\sigma^2(F) + 0.000\,5|F|^2]$ giving a satisfactory analysis of variance. The final electron-density difference synthesis showed no peaks > 1.95 or < -1.26 e Å^{-3}, the largest lying close to the metal atoms. All calculations were performed on a Data General Eclipse Computer with the SHELXTL system of programs.[22] Scattering factors with corrections for anomalous dispersion were taken from ref. 24. The atom co-ordinates are given in Table 5.

Additional material available from the Cambridge Crystallographic Data Centre comprises H-atom co-ordinates, thermal parameters, and remaining bond lengths and angles.

Acknowledgements

We thank the USAF Office of Scientific Research (Grant 86-0125) for partial support, and Dr. J. A. K. Howard for assistance with the low-temperature *X*-ray data collection.

References

1 Part 87, S. J. Crennell, D. D. Devore, S. J. B. Henderson, J. A. K. Howard, and F. G. A. Stone, *J. Chem. Soc., Dalton Trans.*, 1989, 1363.
2 D. D. Devore, J. A. K. Howard, J. C. Jeffery, M. U. Pilotti, and F. G. A. Stone, *J. Chem. Soc., Dalton Trans.*, 1989, 303 and refs. therein.
3 M. Green, J. A. K. Howard, A. P. James, C. M. Nunn, and F. G. A. Stone, *J. Chem. Soc., Dalton Trans.*, 1987, 61.
4 (*a*) M. Green, J. A. K. Howard, A. N. de M. Jelfs, O. Johnson, and F. G. A. Stone, *J. Chem. Soc., Dalton Trans.*, 1987, 73; (*b*) M. Green, J. A. K. Howard, A. P. James, A. N. de M. Jelfs, C. M. Nunn, and F. G. A. Stone, *ibid.*, p. 81; (*c*) F-E. Baumann, J. A. K. Howard, R. J. Musgrove, P. Sherwood, and F. G. A. Stone, *ibid.*, 1988, 1891.
5 (*a*) F-E. Baumann, J. A. K. Howard, R. J. Musgrove, P. Sherwood, and F. G. A. Stone, *J. Chem. Soc., Dalton Trans.*, 1988, 1879; (*b*) M. J. Attfield, J. A. K. Howard, A. N. de M. Jelfs, C. M. Nunn, and F. G. A. Stone, *ibid.*, 1987, 2219.
6 M. Green, J. A. K. Howard, A. P. James, A. N. de M. Jelfs, C. M. Nunn, and F. G. A. Stone, *J. Chem. Soc., Chem. Commun.*, 1985, 1778.
7 J. P. Collman and W. R. Roper, *Adv. Organomet. Chem.*, 1968, **7**, 54.
8 F-E. Baumann, J. A. K. Howard, R. J. Musgrove, P. Sherwood, M. A. Ruiz, and F. G. A. Stone, *J. Chem. Soc., Chem. Commun.*, 1987, 1881.
9 S. J. Dossett, A. F. Hill, J. C. Jeffery, F. Marken, P. Sherwood, and F. G. A. Stone, *J. Chem. Soc., Dalton Trans.*, 1988, 2453.
10 J. R. Shapley, S. J. Hardwick, D. S. Foose, G. D. Stucky, M. R. Churchill, C. Bueno, and J. P. Hutchinson, *J. Am. Chem. Soc.*, 1981, **103**, 7383.
11 M. J. Breen, P. M. Shulman, G. L. Geoffroy, A. L. Rheingold, and W. C. Fultz, *Organometallics*, 1984, **3**, 782.
12 J. A. Abad, L. W. Bateman, J. C. Jeffery, K. A. Mead, H. Razay, F. G. A. Stone, and P. Woodward, *J. Chem. Soc., Dalton Trans.*, 1983, 2075.
13 M. R. Churchill, J. C. Fettinger, W. M. Rees, and J. D. Atwood, *J. Organomet. Chem.*, 1986, **301**, 99 and refs. therein.
14 M. D. Fryzuk, P. A. MacNeil, and S. J. Rettig, *J. Am. Chem. Soc.*, 1985, **107**, 6708.
15 G. R. Clark, W. R. Roper, and A. H. Wright, *J. Organomet. Chem.*, 1982, **236**, C7.
16 R. T. Baker, R. E. King, C. Knobler, C. A. O'Con, and M. F. Hawthorne, *J. Am. Chem. Soc.*, 1978, **100**, 8266; P. E. Behnken, T. B. Marder, R. T. Baker, C. B. Knobler, M. R. Thompson, and M. F. Hawthorne, *ibid.*, 1985, **107**, 932.

17 D. M. P. Mingos, M. I. Forsyth, and A. J. Welch, *J. Chem. Soc., Dalton Trans.*, 1978, 1363.
18 R. H. Crabree, P. C. Demon, D. Eden, J. M. Mikelcic, C. A. Parnell, J. M. Quirk, and G. E. Morris, *J. Am. Chem. Soc.*, 1982, **104**, 6994.
19 D. D. Devore, C. Emmerich, J. A. K. Howard, and F. G. A. Stone, *J. Chem. Soc., Dalton Trans.*, 1989, 797.
20 M. Green, T. A. Kuc, and S. H. Taylor, *J. Chem. Soc. A*, 1971, 2334.
21 G. Mestroni, A. Camus, and G. Zassinovich, *J. Organomet. Chem.*, 1974, **73**, 119.
22 G. M. Sheldrick, SHELXTL programs for use with the Nicolet *X*-Ray System, Revision 5.1, 1985.
23 P. Sherwood, BHGEN, a program for the calculation of idealised H-atom positions for a *nido*-icosahedral carbaborane fragment, 1986.
24 'International Tables for *X*-Ray Crystallography,' Kynoch Press, Birmingham, 1974, vol. 4.

Received 28*th September* 1988; *Paper* 8/03840F